

Integrated fluorescent light source for optofluidic applications

Dmitri V. Vezenov, Brian T. Mayers, Daniel B. Wolfe, and George M. Whitesides

Citation: [Applied Physics Letters](#) **86**, 041104 (2005); doi: 10.1063/1.1850610

View online: <http://dx.doi.org/10.1063/1.1850610>

View Table of Contents: <http://scitation.aip.org/content/aip/journal/apl/86/4?ver=pdfcov>

Published by the [AIP Publishing](#)

Articles you may be interested in

[Tunable on chip optofluidic laser](#)

Appl. Phys. Lett. **107**, 211105 (2015); 10.1063/1.4936235

[Compact resonant integrated microfluidic refractometer](#)

Appl. Phys. Lett. **88**, 093513 (2006); 10.1063/1.2181204

[Microfluidic detection and analysis by integration of thermocapillary actuation with a thin-film optical waveguide](#)

Appl. Phys. Lett. **86**, 184101 (2005); 10.1063/1.1922075

[Bottom-up soft-lithographic fabrication of three-dimensional multilayer polymer integrated optical microdevices](#)

Appl. Phys. Lett. **85**, 3005 (2004); 10.1063/1.1802380

[Integrated optical measurement system for fluorescence spectroscopy in microfluidic channels](#)

Rev. Sci. Instrum. **72**, 229 (2001); 10.1063/1.1326929

The image shows the cover of the journal Applied Physics Reviews. It features a 3D diagram of a layered structure with various components labeled. The AIP logo is in the top left corner, and the title 'Applied Physics Reviews' is in the top right corner. The background is a dark blue with a glowing light effect.

NEW Special Topic Sections

NOW ONLINE
Lithium Niobate Properties and Applications:
Reviews of Emerging Trends

AIP Applied Physics Reviews

Integrated fluorescent light source for optofluidic applications

Dmitri V. Vezenov, Brian T. Mayers, Daniel B. Wolfe, and George M. Whitesides^{a)}
Department of Chemistry and Chemical Biology, Harvard University, 12 Oxford Street, Cambridge, Massachusetts 02138

(Received 4 August 2004; accepted 1 December 2004; published online 18 January 2005)

This letter describes a simple fluidic light source for use “on-chip” in integrated microsystems. It demonstrates the feasibility of light sources based on liquid-core, liquid-cladding (L^2) microchannel waveguides, with liquid cores containing fluorescent dyes. These fluorescent light sources, using both miscible and two-phase systems, are tunable in terms of the beam size, intensity and spectral content. The observed output intensity from fluorescent L^2 light sources is comparable to standard fiber optic spectrophotometer light sources. Integration of fluorescent light sources during device fabrication removes both the need for insertion and alignment of conventional, optical-fiber light sources and the constraints on channel size imposed by fiber optics, albeit at the cost of establishing a microfluidic infrastructure. © 2005 American Institute of Physics. [DOI: 10.1063/1.1850610]

This letter describes a simple, fluidic light source that can be integrated “on-chip” for use in microsystems.¹ We use a liquid core, liquid-cladding (L^2) waveguide, in which the core liquid contains a fluorescent dye. Liquid-core waveguiding has been used previously to increase the optical path in sensing applications;^{2–9} here, we demonstrate the feasibility of low-power light sources based on liquid-core microchannel waveguides. In this system, light emission, collection and propagation all occur within the liquid core.

L^2 waveguides are microfluidic systems in which a flow of a liquid with low index of refraction (the cladding) envelops a flow of another liquid with higher index of refraction (the core). At low Reynolds numbers (Re) in a single channel, these two liquids flow laminarily.¹⁰ The stable, smooth interface between the two liquids makes it possible to guide light in the high-index liquid stream. The L^2 system has three characteristics that may make it preferable to both solid-core/solid-cladding, and liquid-core/solid-cladding waveguides in some applications: (i) the optical smoothness of the L^2 interface, (ii) the ability to control the numerical aperture (refractive index contrast), geometry and position of the waveguide; and (iii) the ability to choose the organic fluorophores used, and to change them dynamically.

Figure 1 shows the design of the microfluidic device we used to evaluate the performance and characteristics of the L^2 fluorescent light source. Microchannels were fabricated in poly(dimethylsiloxane) (PDMS) using replica molding.¹¹ A section of the channel (~4 mm) was irradiated (optically pumped) with a collimated beam from a quartz halogen lamp (150 W, Cuda Fiber Optic Light Source, Model I-150) perpendicular to the long axis of the channel. Fluorescent light output was collected at a T junction at the end of the microfluidic channel; this T formed the exit aperture of the waveguide.

The amount of light that will be captured/guided by the liquid core is strongly dependent on the contrast in refractive index between the core and the cladding, $\Delta n = n_{\text{core}} - n_{\text{cladding}}$ (where n is the index of refraction). In an optically smooth PDMS microchannel completely filled with an ethylene gly-

col (EG) solution of a fluorescent dye, 1% of the light that is emitted isotropically from the dye will, in theory, be guided (the captured fraction is $\Delta n / (2n_{\text{core}})$ (see EPAPS Ref. 18)). The light transmitted through the waveguide will, in practice, suffer losses due to absorption (e.g., by the dye itself; that is, by self-absorption) and scattering (e.g., from the roughness in the sidewalls of the PDMS channel). The introduction of a liquid cladding produces an optically smooth interface, and allows dynamic control over the refractive index contrast. An EG/water L^2 waveguide, for example, can in principle capture $\Delta n / (2n_{\text{core}}) = 3.5\%$ of the emitted light. The liquid cladding also allows control of other characteristics of the waveguide, since the free energy of its interfaces with PDMS, and with the liquid core, can be tuned to control the shape of the core, and consequently its modal content.⁹ The composition and miscibility of the core and cladding liquids, and the diffusion constants of components of the system, can be manipulated to determine the shape of the optical interface.

Our prototype L^2 system consisted of EG ($n_D = 1.432$) containing rhodamine 6G (Rh6G, 0.1–10 mM) as the core stream, and water ($n_D = 1.331$) as the cladding stream. We chose EG for its relatively high refractive index (higher than PDMS, $n_D = 1.406$) and because it is a good solvent for many fluorescent dyes.¹² Miscibility of EG and water ensures a stable interface in a laminar flow regime, although mutual diffusion of the two liquids (and the dye) leads to changes in the refractive index contrast (and dye distribution) along the length of the channel.

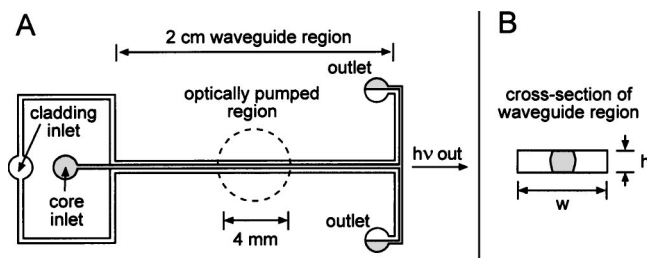


FIG. 1. (A) Top-view scheme for the L^2 fluorescent light source based on microfluidic channels in PDMS; (B) the cross section of the device that was used for imaging onto the photodiode and CCD camera was $50 \mu\text{m} \times 200 \mu\text{m}$ ($h \times w$). Larger microchannels $\sim 125 \mu\text{m} \times 500 \mu\text{m}$ ($h \times w$) were used for end-coupling the device to a spectrometer with optical fiber.

^{a)} Author to whom correspondence should be addressed; electronic mail: gwhitesides@gmwhgroup.harvard.edu

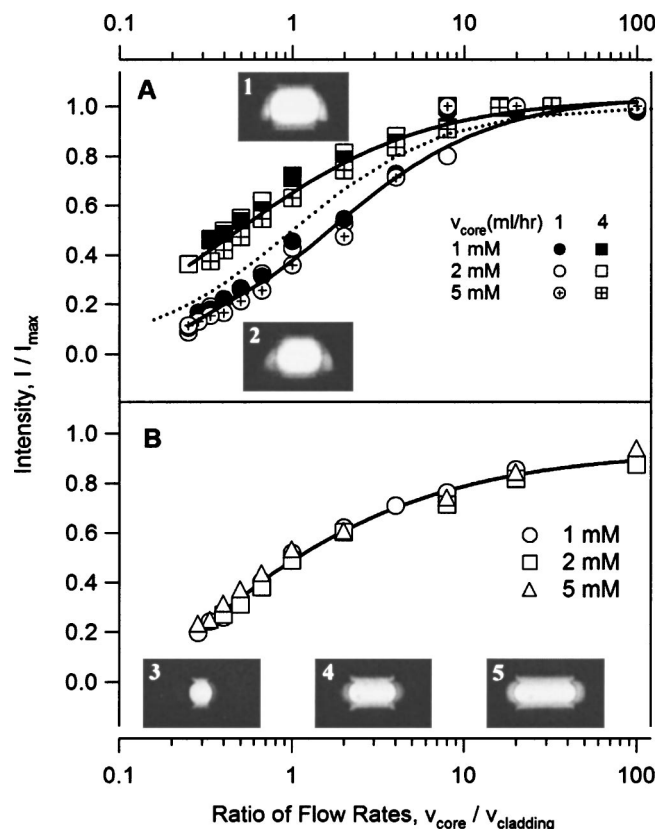


FIG. 2. Optical power output of Rh6G fluorescent L^2 light source with diffusive (A, EG water) and immiscible (B, EG silicone oil) core-cladding interfaces. The dashed curve in (A) is the theoretical intensity based on the volume of the pumped region at different flow rate ratios. Other curves are drawn to guide the eye. Spatial intensity distributions of the two systems were recorded with a CCD camera at some representative flow rate ratios ($v_{\text{core}}:v_{\text{cladding}}$ in mL/h): (1) 4:4; (2) 1:1; (3) 1:0.2; (4) 1:2; and (5) 1:20.

Figure 2(a) shows a plot of normalized optical power (I/I_{max}) versus the ratio of volumetric flow rates ($v_{\text{core}}/v_{\text{cladding}}$, syringe-pump, pressure-driven flow) for the EG/water system. We measured the intensity of the output light by imaging the exit aperture of the microchannel L^2 waveguide with a microscope objective (numerical aperture, $\text{NA}=0.25$) onto a Si photodiode (ThorLabs, NJ). In this figure, we took the maximum intensity to be that observed when the channel was completely filled with the Rh6G/EG solution. Cross sections of the same system were imaged onto a CCD camera and are also shown for the case of $v_{\text{core}}=v_{\text{cladding}}=1$ and 4 mL/h. We note that the optical waveguide is formed by two separate sets of interfaces: (1) EG/water on the sides, and (2) EG/PDMS on the top and bottom.

The intensity of the output increased with increasing core width (determined by the ratio of the flow rates). We expect, for a perfectly loss-less system, that intensity should be directly proportional to the amount of fluorophore in the optically pumped zone (that is, to its concentration, and to the cylindrical volume defined by the cross section of the core and the length of the optically pumped zone). This assumption is consistent with the fact that intensities observed for different concentrations of the dye fall onto the same master curve when normalized for the maximum intensity at a given concentration. For a fixed concentration, the total amount of fluorophore illuminated should be independent of the flow rate. There is, however, a pronounced effect of the flow rate on the optical output. The dashed curve in Fig. 2(a)

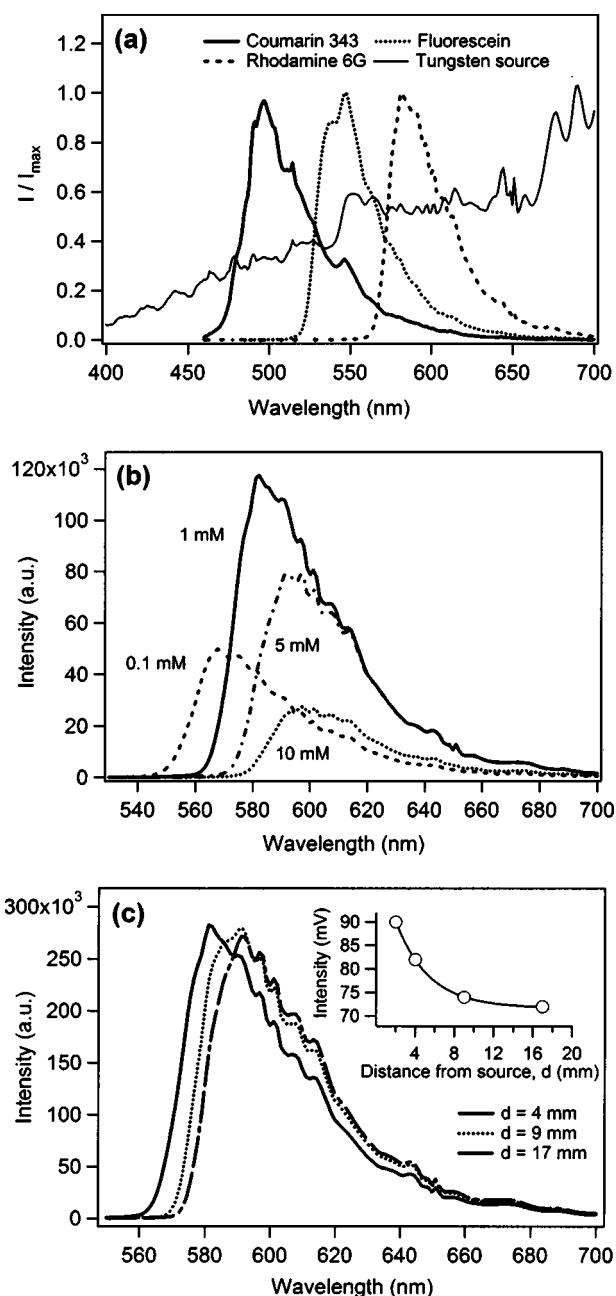


FIG. 3. (A) Emission spectra of the L^2 (core: EG/cladding: water) fluorescent waveguide light sources containing different dyes (the raw peak intensities were within 30% of each other before normalization). The spectra were obtained by coaxially end coupling 105 μm core multimode silica optical fiber (125 μm total diameter) at the T terminus of the microfluidic channel. A spectrum of the tungsten light source of the spectrometer coupled directly to the spectrometer input by the same type of the fiber is shown for comparison. The fine structure in the spectra reflects the throughput characteristics of the fiber optics; (B) emission spectra of the Rh6G microfluidic light source observed for different concentrations of the fluorophore. The optical pumping region was centered 4 mm away from the waveguide output; (C) shift in emission maxima of the Rh6G microfluidic light source due to variation in the propagation distance, d , within the L^2 waveguide. Inset: optical power vs distance between the center of the optically pumped region and L^2 waveguide output. After initial quick falloff due to self-absorption, the optical power losses are <0.2 dB/cm.

represents the theoretical intensity, which should be directly proportional to the volume of the pumped region at different ratios of flow rates (extrapolated from I_{max}). At low flow rates ($v_{\text{core}}=1$ mL/h), the effects of diffusion reduce the output by decreasing the refractive index contrast⁹ and leading to a smaller effective NA of the waveguide. Conversely, at

flow rates above a critical diffusion limit, the high optical contrast achieved by introducing a low index can improve the efficiency of a liq/PDMS system by more than a factor of two with respect to the theoretical curve.

L^2 waveguides based on *immiscible* liquids eliminate issues associated with diffusion. Silicone oil (DC200, $n_D = 1.401$, 10 mPa s, Fluka) was used as the cladding liquid to demonstrate this fact. Figure 2(b) plots the normalized intensity versus the ratio of flow rates for a system comprising Rh6G EG and silicone oil. This curve was invariant to changes in the total flow rate. Hydrophobic cladding streams are attractive because they fully wet the walls of the PDMS microchannel, and, thus, provide stable multiphase flows and cross sections that are more rounded than those derived with miscible streams [Fig. 2(b) insets].

We characterized the system spectroscopically by end coupling the output of the microfluidic system to a UV-Vis spectrometer (SI Photonics, Inc.) using an optical fiber. Figure 3(a) displays the normalized spectra of three EG/water L^2 waveguide systems, each containing different dyes with emission in the visible regime: Rh6G ($\lambda_{\max} = 582$ nm), fluorescein ($\lambda_{\max} = 547$ nm), and coumarin 343 ($\lambda_{\max} = 497$ nm). For reference, the same graph shows the output of a standard fiber-coupled tungsten lamp source (normalized to the I_{\max} of the Rh6G). The dye can be switched in real time to cover the spectral range of interest without fabrication of a new device. The fluorescent waveguide is not susceptible to bleaching, because dye solution is constantly replenished.

Figure 3(b) displays the spectra for the Rh6G system at various dye concentrations. The apparent redshift in λ_{\max} of emission with increasing concentration, from 568 nm at 0.1 mM to 592 nm at 5 mM, is due to the small Stokes shift of Rh6G (~ 30 nm) and the large spectral overlap in absorption and emission. At concentrations > 0.1 mM, there is a significant component of self-absorption. In addition, at concentrations ≥ 10 mM, intermolecular self-quenching rapidly decreased output intensity. An apparent redshift was also seen when the optically pumped zone was moved along the waveguide axis away from the output, increasing the pathlength for absorption [Fig. 3(c)]. The reduction in the output intensity did not exceed 20% for paths as long as 2 cm. Self-quenching should be less pronounced for dyes with larger Stokes shifts.¹³ We note that concentrations of ~ 1 mM of typical fluorophores (extinction coefficients $\sim 10^5$ M⁻¹ cm⁻¹) yield optical densities of ~ 1 in a 100 μ m high channel, and thus provide optimal absorption of incident light in microchannels.

The power density generated by these systems was on the order of 250 W/m² when pumped using a standard 150 W tungsten-halogen light source. While we estimate that the overall efficiency of the Rh6G waveguide is on the order of 0.01% (the ratio of power-in available for absorption to the microchannel to power-out from the waveguide: ~ 20 and 0.002 mW, respectively), the optical power output could be further increased by improving the coupling of the pump light sources to the dye-containing waveguide. For most applications, these refinements will be unnecessary, since the available optical power is comparable to, or exceeds, that available from conventionally coupled fiber optic light sources for spectroscopy (SI Photonics Spectrophotometer, Model 430).

This L^2 fluorescent light source has four useful characteristics: (1) The system generates output intensity compa-

rable to standard fiber-optic spectrophotometer-based light sources, while removing the need for manual insertion/alignment of the optical fiber, and the constraints on size that are typically imposed by such fibers. (2) It also has the tunability/flexibility that characterize L^2 waveguide systems in general.⁹ In addition to the ability to select core and cladding fluids, there is a wide range of potential fluorescent dyes, (3) microfluidic light sources should, in principle, eliminate the need for careful alignment of external radiation sources for microfluidic devices (a major drawback for fiber-optic-coupled light sources), because the fluidic light sources are prealigned in the course of design and fabrication. (4) The L^2 systems are easily fabricated in polymers using the techniques of rapid prototyping, and give high degree of control over optical surfaces in the microchannels.^{11,14} The disadvantage of these systems is the requirement to manipulate liquids using pumps and reservoirs. This infrastructure should, however, already be available for applications based on the microfluidic devices, and the fabrication process is the same as that of the device itself.

As bioanalytical systems become smaller,¹⁵⁻¹⁷ they continue to rely on optical detection. Optical methods usually require bulky and costly components, and their precise alignment. The fluorescent waveguide light source presented here can be integrated into microanalytical devices and has characteristics similar to those encountered in a typical setup with a fiber optic spectrometer. These characteristics can be easily adjusted due to the fluid nature of the waveguide.

This work was supported by DARPA as a Subaward from the California Institute of Technology. It used facilities of the MRSEC and NSEC, both supported by NSF. We thank Richard S. Conroy for helpful discussions.

¹E. Verpoorte, *Lab Chip* **3**, 42N (2003).

²R. J. Dijkstra, C. J. Slooten, A. Stortelder, J. B. Buijs, F. Ariese, U. A. T. Brinkman, and C. Gooijer, *J. Chromatogr., A* **918**, 25 (2001).

³P. Dress and H. Franke, *Appl. Phys. B: Lasers Opt.* **63**, 12 (1996).

⁴A. Hanning, J. Westberg, and J. Roeraade, *Electrophoresis* **21**, 3290 (2000).

⁵Z. Liu and J. Pawliszyn, *Anal. Chem.* **75**, 4887 (2003).

⁶J. A. Olivares, P. C. Stark, and P. Jackson, *Anal. Chem.* **74**, 2008 (2002).

⁷O. J. A. Schueller, X.-M. Zhao, G. M. Whitesides, S. P. Smith, and M. Prentiss, *Adv. Mater. (Weinheim, Ger.)* **11**, 37 (1999).

⁸S.-L. Wang, X.-J. Huang, Z.-L. Fang, and P. K. Dasgupta, *Anal. Chem.* **73**, 4545 (2001).

⁹D. B. Wolfe, R. S. Conroy, P. Garstecki, B. T. Mayers, M. A. Fischbach, K. E. Paul, M. Prentiss, and G. M. Whitesides, *Proc. Natl. Acad. Sci. U.S.A.*, **101**, 1243 (2004).

¹⁰H. A. Stone, A. D. Stroock, and A. Ajdari, *Annu. Rev. Fluid Mech.* **36**, 381 (2004).

¹¹J. C. McDonald and G. M. Whitesides, *Acc. Chem. Res.* **35**, 491 (2002).

¹²M. Maeda, *Laser Dyes: Properties of Organic Compounds for Dye Lasers* (Academic, New York, 1984).

¹³I. B. Berlman, *Handbook of Fluorescence Spectra of Aromatic Molecules*, 2nd ed. (Academic, New York, 1971).

¹⁴Y. Xia and G. M. Whitesides, *Annu. Rev. Mater. Sci.* **28**, 153 (1998).

¹⁵T. Vilkner, D. Janasek, and A. Manz, *Anal. Chem.* **76**, 3373 (2004).

¹⁶S. Mouradian, *Curr. Opin. Chem. Biol.* **6**, 51 (2002).

¹⁷A. Kopf-Sill, *Lab Chip* **2**, 42N (2002).

¹⁸See EPAPS Document No. E-APPLAB-86-056502 for derivation of the expression for the fraction of the fluorescence guided by the L^2 waveguide. A direct link to this document may be found in the online article's HTML reference section. The document may also be reached via the EPAPS homepage (<http://www.aip.org/pubservs/epaps.html>) or from <ftp://p.aip.org> in the directory/epaps/. See the EPAPS homepage for more information.